Broad-Band Uniplanar Hybrid-Ring and Branch-Line Couplers

Chien-Hsun Ho, Lu Fan, and Kai Chang, *Fellow, IEEE*

Abstract—**Novel uniplanar 180° and 90° hybrids suitable for MIC and MMIC are described. The new uniplanar crossover hybrid-ring magic-T coupler using a coplanar waveguide (CPW) and slotline provides substantially improved amplitude and phase characteristics over a broad bandwidth compared to conventional microstrip hybrid-ring couplers. Experimental results show that the uniplanar crossover hybrid-ring coupler has a bandwidth of more than one octave from 2 to 4 GHz with ±0.4 dB power dividing balance and ±1° phase balance. A uniplanar two-branch directional coupler using a coupled rectangular slotline ring has also been developed that has over 20 dB isolation over a bandwidth of more than 40% centered at 3 GHz with ±1 dB power dividing balance. To fully utilize the advantages of uniplanar structures, transitions from CPW to slotline and coplanar strip (CPS) using uniform and nonuniform CPWs, slotlines, or CPSs are discussed. These transitions are uniplanar and simple to fabricate. No via holes are needed for ground connections, and integration with solid-state devices is easy. A pair of broad-band transitions using CPW shorts and slotline radial stubs is demonstrated with a 1 dB bandwidth of more than 5.2:1. The CPW–CPS transition shows a 1 dB bandwidth of more than two octaves.**

I. Introduction

HYBRID couplers are indispensable components used in various MIC applications such as balanced mixers, balanced amplifiers, frequency discriminators, phase shifters, and feeding networks in antenna rays. Some of the more commonly used are 180° hybrid rings and 90° branch-line couplers. Rat-race hybrid rings [1], reverse-phase hybrid rings [2], [3], and crossover hybrid rings [4] are well-known examples of 180° hybrid rings. Some other improved bandwidth hybrid rings have also been reported in [5]–[6]. 90° branch-line couplers have been analyzed in [7]–[12]. A computer-aided design technique that is suitable for the optimum design of multisection branch-line couplers was described in [13]. Some other optimized methods that included compensation for the junction discontinuities were also reported [14]–[17]. Another class of MIC 90° branch-line coupler using a combination of microstrip lines and slotlines was proposed in [18] and optimized in [19]–[24].

Manuscript received March 23, 1993; revised June 9, 1993. This work was supported in part by the U.S. Army Research Office and the State of Texas Higher Education Coordinating Board's Advanced Technology Program.

The authors are with the Department of Electrical Engineering, Texas A&M University, College Station, TX 77843.

IEEE Log Number 9213007.

In recent years, the uniplanar transmission line has emerged as an alternative to microstrip in planar microwave integrated circuits. The uniplanar MIC does not use the back side of the substrate, and allows easy series and shunt connections of passive and active solid-state devices. Use of the uniplanar structures also circumvents the need for via holes and reduces processing complexity. Many attractive components using uniplanar structures have been published [25]–[28]. Some circuit configurations about uniplanar 180° and 90° hybrids were also proposed in [29]–[33].

This paper first discusses the fundamental transition circuits from coplanar waveguides to slotlines and coplanar strips. A broad-band uniplanar hybrid-ring coupler is demonstrated for use at 2–4 GHz. Experimental results show a usable bandwidth of more than one octave. A uniplanar branch-line coupler using a coupled rectangular slotline ring is also developed that provides substantially improved broad-band amplitude and phase characteristics when compared to conventional microstrip branch-line couplers.

II. Transitions Between Uniplanar Transmission Lines

Coplanar waveguide (CPW), coplanar strip (CPS), and slotline are the fundamental transmission lines in uniplanar MIC. They allow easy series and shunt device mounting, easy ground connections, and simple fabrication processes. These characteristics make CPW, CPS, and slotline important in microwave and millimeter-wave integrated circuit designs. To fully utilize the advantages of uniplanar structures, broad-band transitions of CPW-to-slotline and CPW-to-CPS are necessary.

A. CPW-to-Slotline Transitions

Broad-band transitions from microstrip to slotline have been reported by many authors [34]–[37]. The transitions in [34]–[36] are based on the well-known concept of Marchand baluns [38] and Oltmann's compensated baluns [39]. The transition reported in [37] is based on the strip-slot double junction, and has an improved broad bandwidth up to one decade. Equivalent uniplanar CPW–slotline transitions to microstrip–slotline transitions have also been proposed in [40]–[44]. Although these papers introduce some intuitive approaches for designing CPW–slotline transitions, a systematic description of the design

techniques is still lacking. This section is intended to give a systematic approach to this problem based on experimental investigations. Figs. 1–3 show the CPW–slotline transitions investigated in this paper. The objective of developing the different transitions was to find a best combination of CPW short circuits and slotline open circuits to generate broad-band matching from CPW to slotline. The matching discontinuities are classified as: A: CPW shorts or slotline opens, B: uniform CPW open stubs or slotline short stubs, and C: nonuniform CPW open stubs or slotline short stubs. According to the above classifications, Fig. 1 shows the circuit configurations of TYPE-AB and TYPE-AC. TYPE-BB and TYPE-BC are shown in Fig. 2; TYPE-CB and TYPE-CC are shown in Fig. 3. Compared with microstrip–slotline transitions, the CPW–slotline transitions presented in this paper have the advantages of being uniplanar and easy to integrate with solid-state devices, and they require no via holes for ground connections. Experimental results are given by measuring the insertion loss of one pair of coaxial–CPW transitions, CPW–slotline transitions, and an 8 mm length of slotline section. When testing the transitions, bond wires were soldered to every discontinuity between the CPW and the slotline.

Fig. 1(a) shows the CPW–slotline transition (TYPE-AB) using a CPW short with a $\lambda/4$ slotline short stub. The center conductor strip of the CPW in Fig. 1(a) is connected to one side of the slotline to create the CPW short circuit. Fig. 1(b) shows the transition (TYPE-AC) using a CPW short and a slotline radial stub. The angle of the slotline radial stub in Fig. 1(b) is 90°. The characteristic impedances of Z_{CPW} and Z_s are both 50 Ω. The slotline radial stub is a broad-band open; therefore, the resulting CPW–slotline transition should have broad bandwidth. One important feature of this transition is that the CPW and slotline can be connected without bending the transmission structure. This makes the circuit layout flexible. Fig. 4 shows the experimental insertion loss of the TYPE-AB and TYPE-AC back-to-back transitions with a slotline section. The 1 dB bandwidth of the TYPE-AB back-to-back transition is in the 2.3–3.8 GHz frequency range. This kind of transition has a bandwidth of less than one octave and is the worst case of the CPW–slotline transitions investigated. The insertion loss of less than 1 dB for the TYPE-AC back-to-back transition is in the 1.1–5.7 GHz frequency range, which is more than 2.3 octaves. The transition shown in Fig. 1(b) gives the best performance in bandwidth.

Fig. 2(a) shows the $\lambda/4$ cross junction of the TYPE-BB CPW–slotline transition. The CPW and slotline in Fig. 2(a) are etched on the same side of the substrate, and they cross each other at right angles. The CPW extends one quarter of a wavelength beyond the slotline and terminates with an open end. Similarly, the slotline extends one quarter of a wavelength beyond the CPW and terminates with a short end. The extensions of CPW and slotline may act as tuning stubs to match the CPW to the slotline. Both characteristic impedances of CPW and slotline in Fig. 2(a)

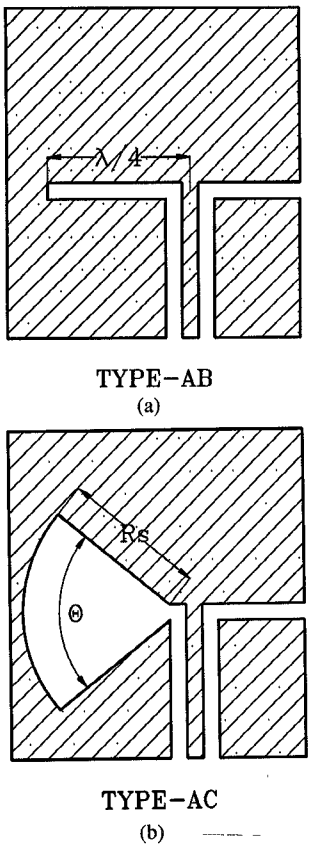

Fig. 1. Circuit configurations of CPW–slotline transitions using a CPW short with a uniform slotline short stub (TYPE-AB) or a nonuniform slotline short stub (TYPE-AC).

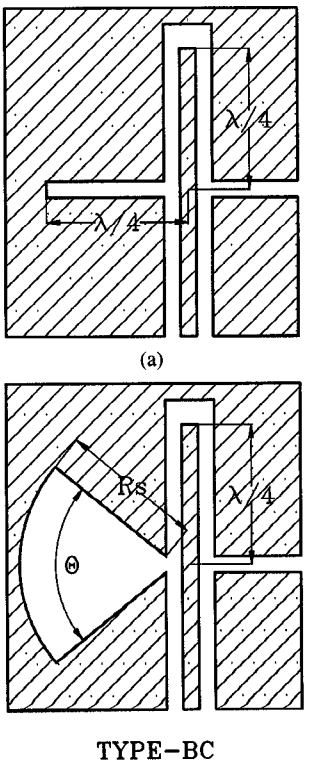

Fig. 2. Circuit configurations of CPW–slotline transitions using a uniform CPW open stub with a uniform slotline short stub (TYPE-BB) or a nonuniform slotline short stub (TYPE-BC).

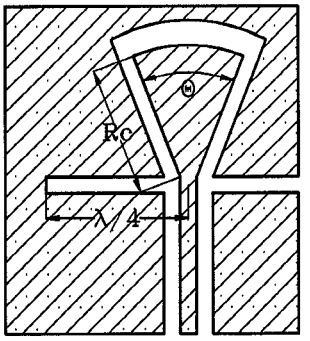

TYPE−CB

(a)

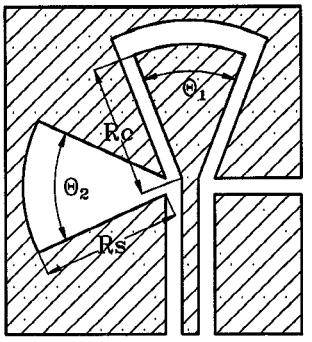

TYPE−CC

(b)

Fig. 3. Circuit configurations of CPW–slotline transitions using a nonuniform CPW open stub with a uniform slotline short stub (TYPE-CB) or a nonuniform slotline short stub (TYPE-CC).

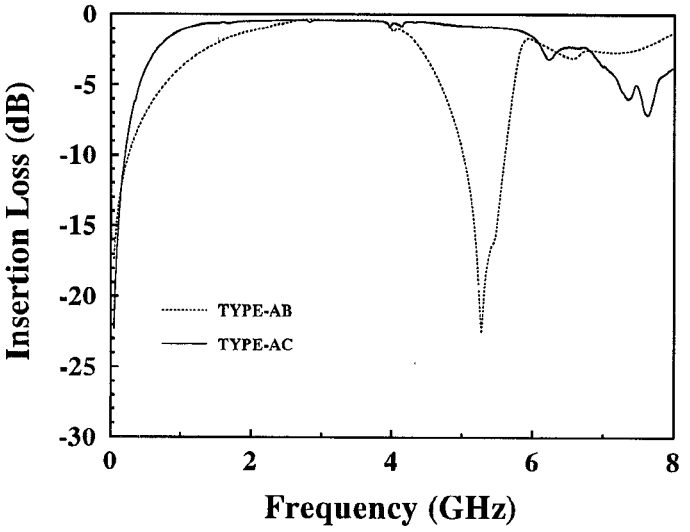

Fig. 4. Measured frequency responses of insertion loss for the CPW-slotline back-to-back transitions of TYPE-AB and TYPE-AC.

are 50 Ω. Fig. 2(b) shows the CPW–slotline transition (TYPE-BC) using a λ/4 CPW open stub and a slotline radial stub. The angle of the slotline radial stub in Fig. 2(b) is 90°. Fig. 5 shows the experimental insertion loss of the TYPE-BB and TYPE-BC back-to-back transitions with a slotline section. The experimental insertion loss of the TYPE-BB back-to-back transition is less than 1 dB in

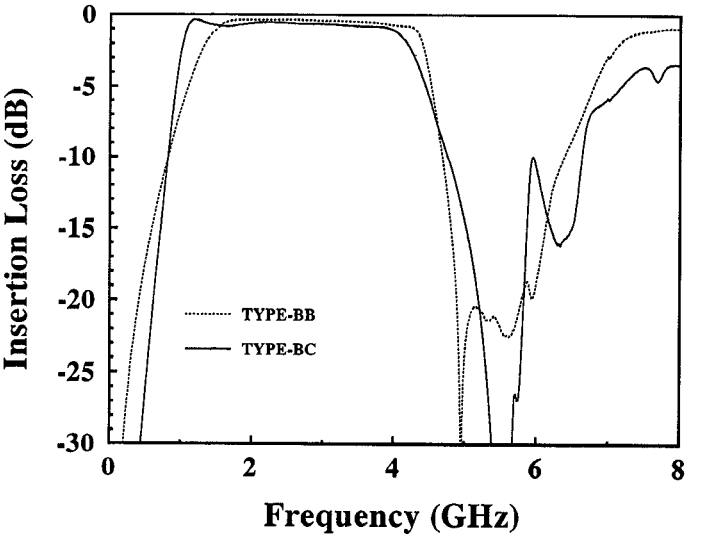

Fig. 5. Measured frequency responses of insertion loss for the CPW-slotline back-to-back transitions of TYPE-BB and TYPE-BC.

the 1.6–3.6 GHz frequency range, which corresponds to a bandwidth of more than one octave. The 1 dB bandwidth of the TYPE-BC back-to-back transition is in the 0.9–3.8 GHz frequency range, which is more than two octaves.

Fig. 3(a) shows the CPW–slotline transition (TYPE-CB) using a CPW radial stub with a λ/4 slotline short stub. Fig. 3(b) shows the CPW–slotline transition (TYPE-CC) using both the nonuniform CPW open and slotline short stubs. The angles of the CPW and slotline radial stubs are both chosen as 45° to avoid interfering with each other. The experimental results of the insertion loss for the back-to-back transitions of TYPE-CB and TYPE-CC are shown in Fig. 6. The 1 dB bandwidth of the TYPE-CB back-to-back transition is in the 1.5–3.8 GHz frequency range; the 1 dB bandwidth of the TYPE-CC back-to-back transition is from 1.5 to 6.0 GHz, which is more than two octaves.

Table I summarizes the combinations and usable 1 dB bandwidth of the CPW-to-slotline transitions shown in Figs. 1–3. From the experimental results, we can conclude the following.

1) The transitions of TYPE-AC, TYPE-BC, and TYPE-CC, which use slotline radial stubs, have broad bandwidths of more than two octaves. This means that: a) slotline open circuits are the dominant factors of designing the broad-band CPW-slotline transitions, and b) slotline radial stubs are good candidates for designing broad-band slotline open circuits.

2) The transitions using virtual CPW shorts (either quarter-wavelength or radial open stubs) have sharp gain slopes. This feature may be used in the design of bandpass filters.

3) The transition of TYPE-AC using a CPW short and a slotline radial stub can be designed without bending the transmission structure. Circuit layout with this transition is flexible.

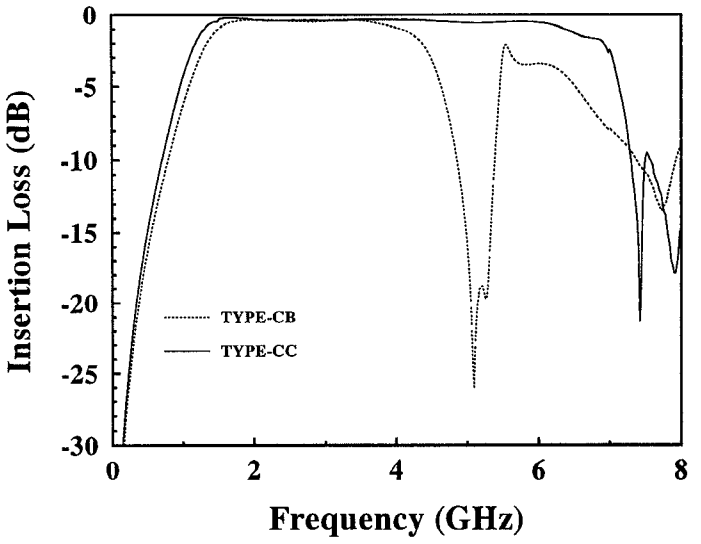

Fig. 6. Measured frequency responses of insertion loss for the CPW-slotline back-to-back transitions of TYPE-CB and TYPE-CC.

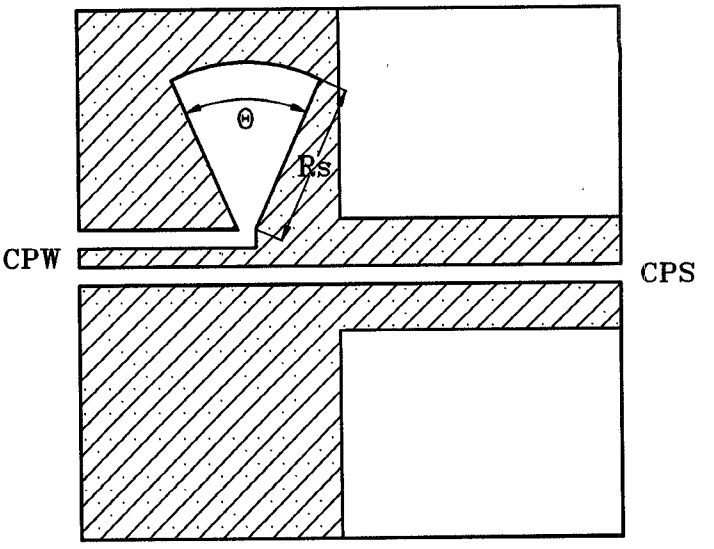

Fig. 7. The CPW–CPS transition configuration.

TABLE I
SUMMARY OF THE COMBINATIONS AND 1 dB BANDWIDTH OF DIFFERENT CPW SHORTS AND SLOTLINE OPENS. (THE INSERTION LOSS INCLUDES TWO COAXIAL-CPW TRANSITIONS, TWO CPW–SLOTLINE TRANSITIONS, AND A SLOTLINE SECTION.)

CPW \ Slotline	Uniform Short Stub	Nonuniform Short Stub
Short	16:1 (TYPE-AB)	5.2:1 (TYPE-AC)
Uniform Open Stub	2.2:1 (TYPE-BB)	4.0:1 (TYPE-BC)
Nonuniform Open Stub	2.5:1 (TYPE-CB)	4.1:1 (TYPE-CC)

4) The transition of TYPE-AC using a CPW short and a slotline radial stub is the best combination for the broadband and low-loss applications. The bandwidth of less than 1 dB insertion loss has been demonstrated more than 5.2:1. The designs and layouts of this type of transition are easy, compact, and flexible. By choosing a proper angle and radius for the slotline radial stub, the bandwidth of the transition can be further improved.

B. CPW-to-CPS Transitions

A wide-band and low return loss transition from microstrip to CPS has been proposed in [45] using an intermediate microstrip line. To design the transition between CPW and CPS, an intermediate slotline section is required. Fig. 7 shows the transition from CPW to CPS with an intermediate slotline section. The intermediate transition from CPW to slotline uses TYPE-AC described in the previous section, which has a 1 dB bandwidth of more than 5.2:1. Fig. 8 shows the frequency responses of insertion loss and return loss for the CPW–CPS transition. The insertion loss of less than 1 dB is in the frequency range from 1.6 to 7.0 GHz, which corresponds to a bandwidth of more than two octaves. The return loss of the CPW–CPS transition is less than −13 dB from 1.6 up to 8 GHz.

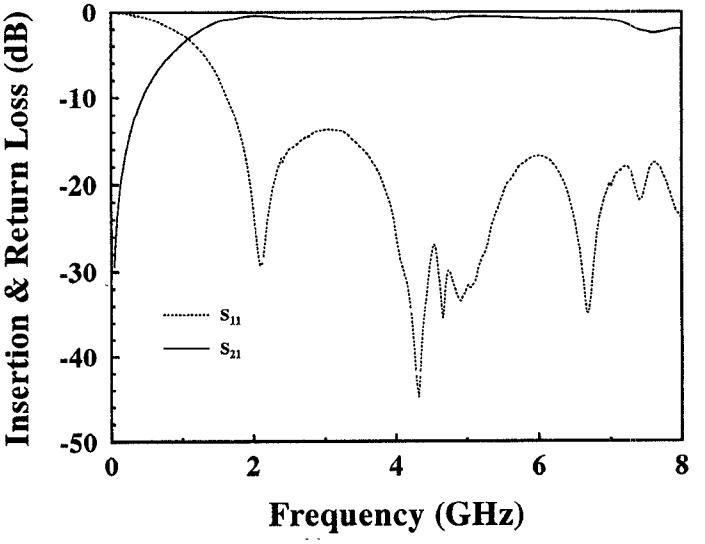

Fig. 8. Measured frequency responses of insertion loss and return loss for the CPW–CPS back-to-back transition.

III. 180° UNIPLANAR HYBRID-RING COUPLERS

The microstrip rat-race hybrid-ring coupler is the basic power divider used in many printed microwave integrated circuits. The 20–25% bandwidth of this coupler limits its applications to narrow-band circuits. Several design techniques have been developed to extend the bandwidth. One technique used a $\lambda/4$ coupled microstrip line section to replace the $3\lambda/4$ section of the conventional $3\lambda/2$ microstrip ring coupler, where λ is the guide wavelength [2]. Although the bandwidth was increased to more than one octave, the difficulty of constructing the coupled microstrip line section, which required short circuits at the ends, limited its use to low frequencies. Another modified version of the microstrip rat-race hybrid-ring substituted a quarter-wavelength slotline section etched on the other

side of the substrate for the phase delay section [3]. Although a bandwidth of two octaves was realized, the two-sided substrate required a more complicated photolithographic process and limited the coupler to low frequencies. Two other approaches [5], [6] used hypothetical ports with matching circuits. This technique achieved a 50% bandwidth; however, the matching circuits described in [5] required very wide microstrip lines and a larger number of different impedances, and the broad-band design technique presented in [6] was useful in the sum mode (in-phase mode) of operation only. Both matching techniques also demanded intensive optimization to obtain good performance.

To extend the bandwidth with a simple design procedure and uniplanar structure, this section presents a new uniplanar hybrid-ring coupler consisting of a slotline ring with one slotline feed and three CPW feeds. The design technique substitutes one reverse-phase slotline T-junction for the conventional rat-race phase delay section. Since the phase reverse of the slotline T-junction is frequency independent, the resulting slotline ring coupler has a broad bandwidth.

Fig. 9(a)–(c) show the three fundamental uniplanar hybrid-ring couplers. The uniplanar rat-race hybrid-ring coupler shown in Fig. 9(a) consists of three quarter-wavelength slotline sections, one phase delay section, and four CPW to slotline T-junctions. The measured results of a uniplanar rat-race hybrid-ring coupler are shown in Fig. 10. The coupler has a bandwidth of 18.6%, with ± 0.3 dB power dividing balance and over 20 dB isolation. The 1.2 dB loss is mainly due to the CPW–slotline T-junction. Fig. 9(b) shows the circuit configuration of the uniplanar reverse-phase hybrid-ring coupler with a $\lambda/4$ coupled-slotline section. Although the coupled-slotline reverse-phase section requires no via holes for the short terminations, it is still difficult to fabricate the very small metal gap between two coupled slotlines with a 3 dB coupling.

Fig. 9(c) shows the physical configuration of the uniplanar crossover hybrid-ring magic-T coupler. The *E*-arm of the uniplanar crossover hybrid ring is fed through a CPW line connected to a broad-band TYPE-AC CPW-to-slotline transition as shown in Fig. 1(b). The slotline T-junction shown in Fig. 9(c) is used as a phase inverter. The impedance of the slotline ring is given by

$$Z_s = \sqrt{2} \cdot Z_{\mathrm{CPW}} \tag{1}$$

where Z_{CPW} is the impedance of the CPW feeds. The radius of the slotline ring is designed by [46]

$$2\pi r = \lambda \tag{2}$$

where λ is the guide wavelength of the slotline ring. According to the above equations, a truly uniplanar crossover hybrid-ring coupler was built on an RT/Duroid 6010.8 ($\epsilon_r = 10.8$) substrate with the following dimensions: 1) substrate thickness: $h = 1.27$ mm, 2) CPW center strip width: $S = 0.51$ mm, 3) CPW gap width: G = 0.25 mm, 4) slotline feed line width: $W_{S1} = 0.1$ mm, 5)

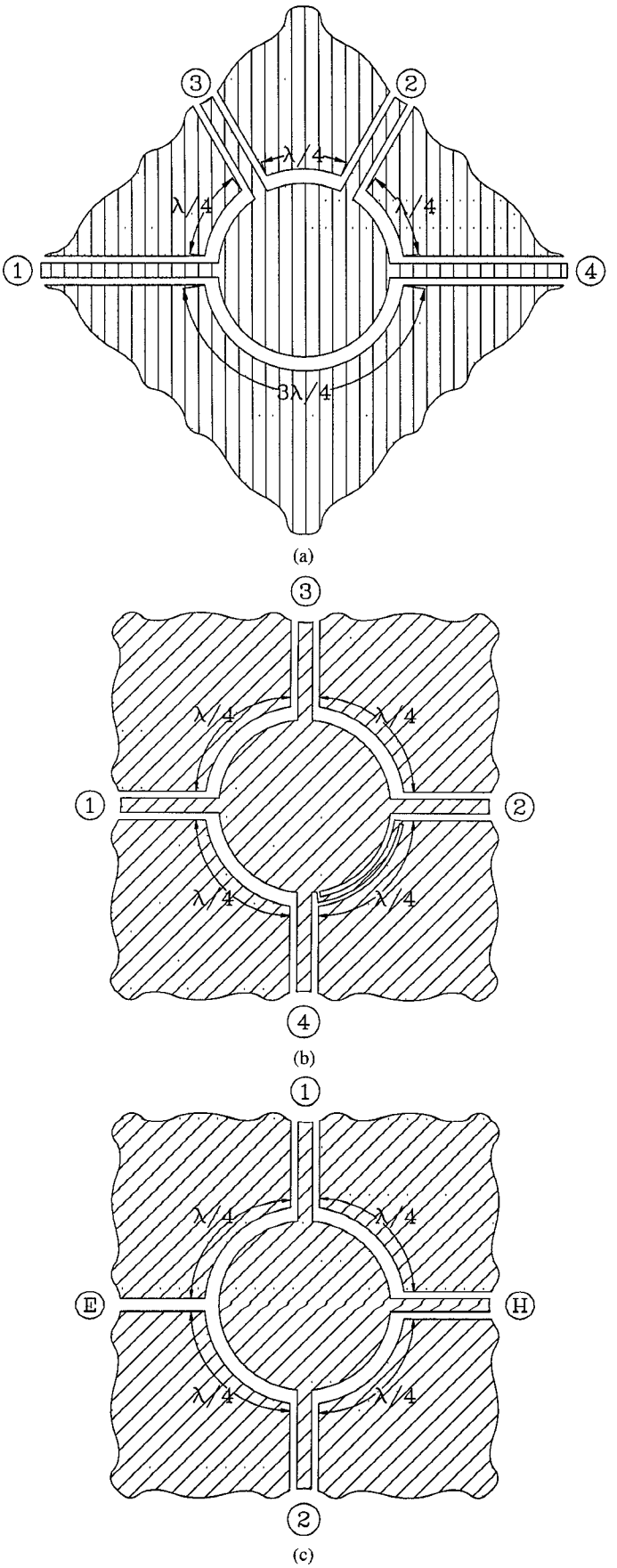

Fig. 9. Circuit configurations of 180° uniplanar hybrid-ring couplers. (a) Rat-race hybrid-ring coupler. (b) Phase-reverse hybrid-ring coupler. (c) Crossover hybrid-ring coupler.

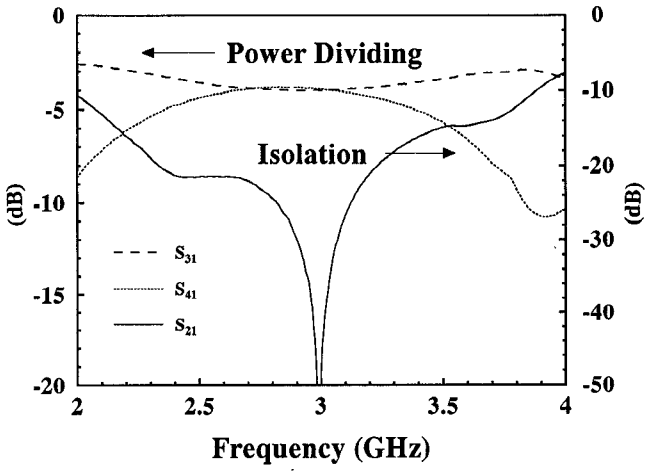

Fig. 10. Measured frequency responses of power dividing and isolation for the uniplanar rat-race hybrid-ring coupler.

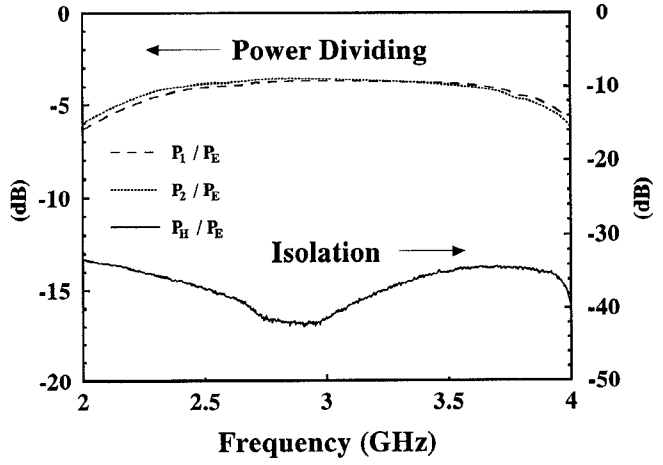

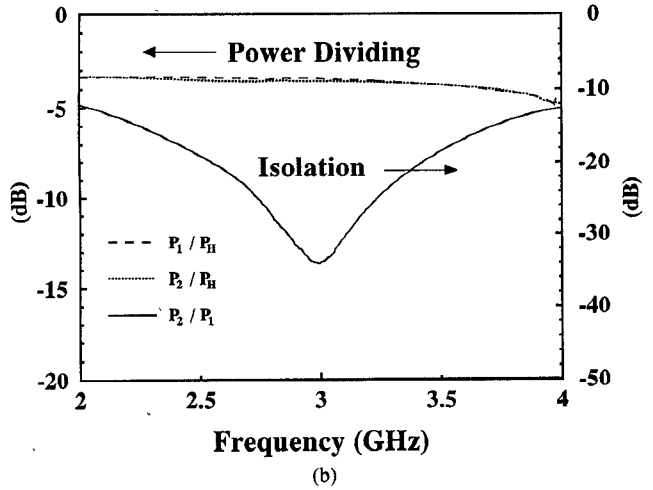

Fig. 11. Measured frequency responses of insertion loss for the uniplanar crossover hybrid-ring coupler. (a) *E*-arm power dividing and isolation. (b) *H*-arm power dividing and isolation.

slotline ring line width: $W_{S2} = 0.43$ mm, and 6) slotline ring radius: $r = 7.77$ mm.

Fig. 11(a) shows the measured insertion loss for the *E*-arm's power dividing balance and the mutual isolation between the *E*-arm and *H*-arm. The power dividing balance of the *E*-arm is less than ± 0.4 dB from 2 to 4 GHz. The insertion loss at the center frequency of 3 GHz is less than 0.6 dB. The isolation between the *E*-arm and *H*-arm is greater than 36 dB. Fig. 11(b) illustrates the measured insertion loss for the *H*-arm's power dividing balance and the mutual isolation between two output balanced arms. The *H*-arm's power dividing balance is less than ± 0.3 dB, and the mutual isolation between the two balanced arms is greater than 12 dB. The insertion loss of the *H*-arm's power dividing is less than 0.5 dB at the center frequency. Fig. 12(a) shows the *H*-arm and *E*-arm's power balances. The *H*-arm's power balance is within ± 0.3 dB and the *E*-arm's power balance is within ± 0.4 dB over the designed frequency band. Fig. 12(b) shows the *H*-arm and *E*-arm's phase balances. The *H*-arm's phase balance is $-0.75° \pm 0.75°$, and the *E*-arm's phase balance is $181° \pm 1°$ from 2 to 4 GHz. The experimental results described above show that the uniplanar crossover hybrid-ring coupler has fairly good power dividing and phase balances compared to the microstrip hybrid-ring couplers.

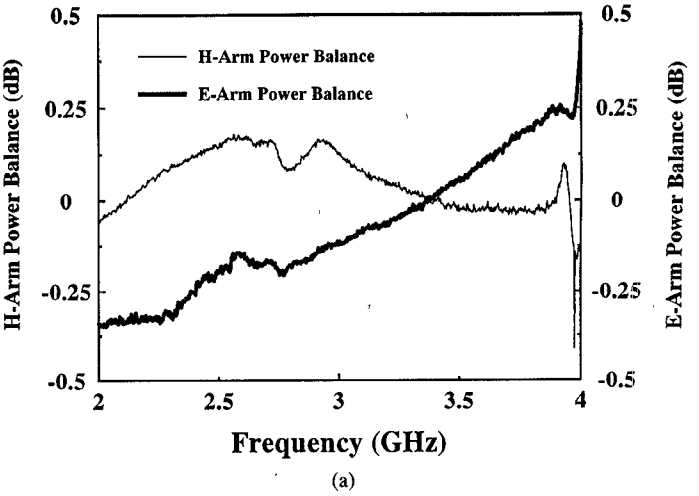

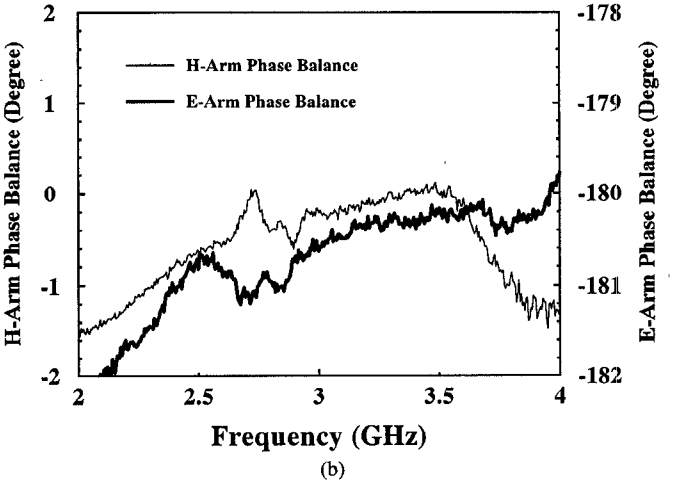

Fig. 12. Power and phase balances of the uniplanar crossover hybrid-ring coupler. (a) Power dividing balances of *H*-arm and *E*-arm. (b) Phase balances of *H*-arm and *E*-arm.

IV. 90° Uniplanar Branch-Line Couplers

The microstrip branch-line coupler is a basic component in applications such as power dividers, balanced mixers, frequency discriminators, and phase shifters. The 10–20% bandwidth of a two-branch coupler limits its applications to narrow-band circuits. Additional coupler sections can overcome this disadvantage [11], but the practical design of couplers with more than four sections is difficult in microstrip [47]. The line widths required by the very high and low impedance branch arms may also create undesirable aspect ratios and junction effects. Several computer optimization techniques have been developed to obtain realizable impedance ranges [13] and predict junction effects [14], [15]; however, realizing even two-branch and three-branch couplers in the millimeter-wave region is still difficult. To overcome these problems, the series T-junctions and signal phase reversals with CPW and slotline were used in MMIC applications. CPW and slotline are very suitable for the designs of balanced circuits in microwave and millimeter-wave MMICs.

This section proposes two new configurations of uniplanar n-branch directional couplers consisting of n-1 rectangular slotline rings coupled with two parallel slotline feeds. Fig. 13(a) shows the circuit configuration of the TYPE-A uniplanar multisection branch-line coupler, and Fig. 13(b) shows the circuit configuration of the TYPE-B uniplanar multisection branch-line coupler. The TYPE-A uniplanar branch-line coupler uses two parallel CPWs for the series arms, and the TYPE-B coupler uses two parallel slotlines as series arms. The shunt branch arms are formed by the n-1 coupled rectangular slotline rings in either TYPE-A or TYPE-B case. For the uniplanar two-branch directional coupler, the configuration of TYPE-A is similar to that of TYPE-B.

Fig. 14 shows the physical configuration of the uniplanar two-branch directional coupler. When a signal is applied to port 1, outputs appear at ports 2 and 3 that are equal in amplitude and differ in phase by 90°. Port 4 represents the isolation arm. The series arms of the coupler are fed through two parallel slotlines coupled by a rectangular slotline ring on two sides. The other two sides of the rectangular slotline ring are shunt branch arms. Bond wires are soldered at the discontinuities between the series and shunt arms to enforce the even mode propagation in the coupled slotlines (CPWs). The corresponding line characteristic impedances of CPW and slotline branch arms for 3 dB coupling, in terms of the termination impedance Z_0, can be expressed as

$$Z_{CPW} = \frac{Z_0}{\sqrt{2}} \tag{3}$$

$$Z_s = Z_0 \tag{4}$$

where Z_{CPW} is the impedance of the CPW series arms and Z_s is the impedance of the slotline shunt branch arms. Ac-

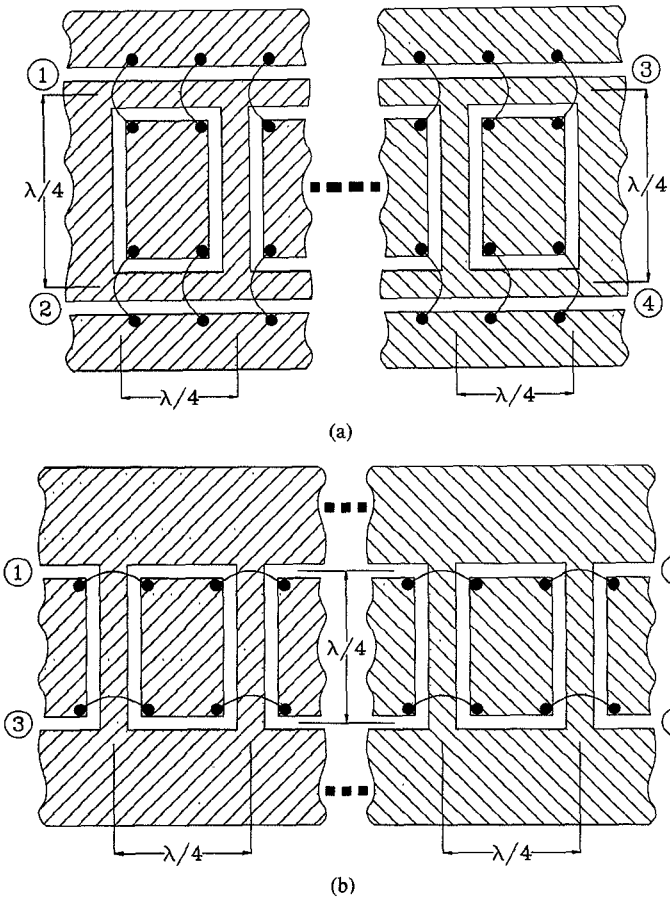

Fig. 13. Circuit configurations of 90° uniplanar branch-line coupler. (a) Multisection TYPE-A uniplanar branch-line coupler. (b) Multisection TYPE-B uniplanar branch-line coupler.

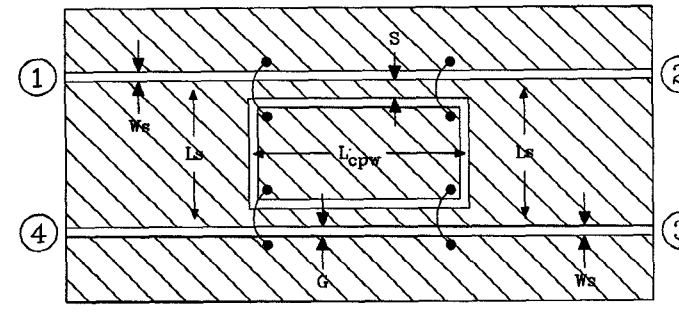

Fig. 14. Circuit configuration of uniplanar two-branch directional coupler.

cording to the above equations, a truly uniplanar two-branch directional coupler was built on an RT/Duroid 6010.8 (ϵ_r = 10.8) substrate with the following dimensions: 1) substrate thickness: h = 1.27 mm, 2) CPW center strip width: S = 0.71 mm, 3) CPW gap width: G = 0.1 mm, 4) rectangular slotline ring line width: W_s = 0.1 mm, 5) length of CPW series arm: L_{cpw} = 10.39 mm, and 6) length of slotline shunt branch: L_s = 7.77 mm.

Figs. 15 and 16 show the measured performances of the fabricated uniplanar two-branch directional coupler. To test the coupler, a wide-band CPW-to-slotline transition was used to connect to ports 1, 2, 3, and 4. The transition

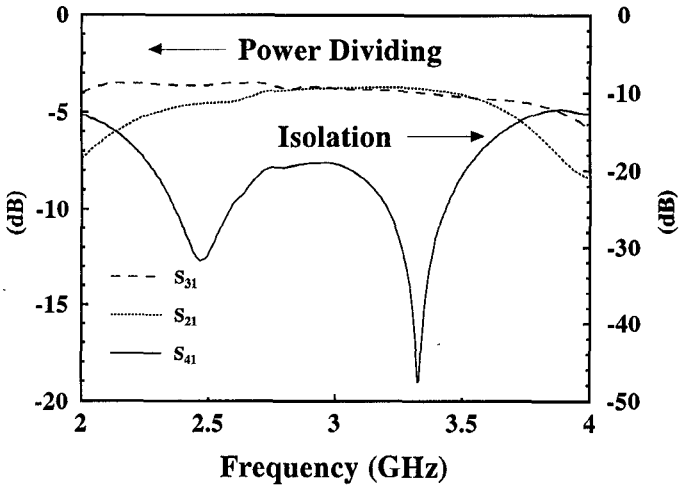

(a)

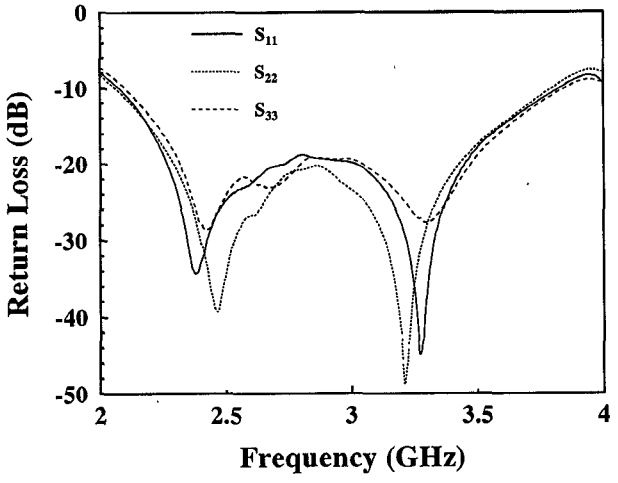

(b)

Fig. 15. Measured frequency responses of (a) power dividing and isolation and (b) return loss for the uniplanar two-branch directional coupler.

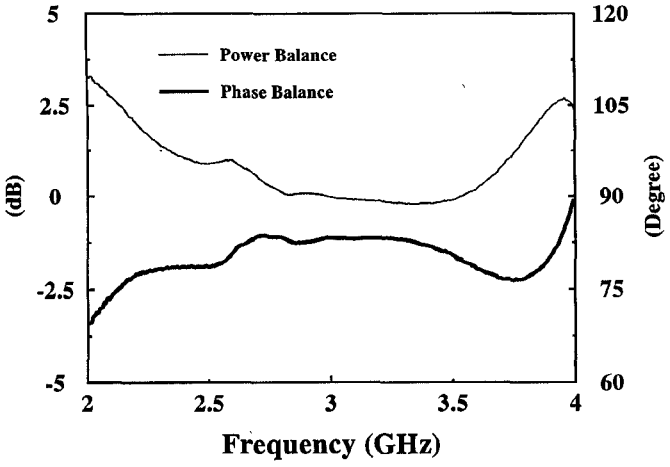

Fig. 16. Power and phase balances of the uniplanar two-branch directional coupler.

consisted of a CPW short and a slotline radial stub which is described as the TYPE-AC transition shown in Fig. 1(b). The measurements were made using standard SMA connectors and an HP-8510 network analyzer. The insertion loss includes two coaxial-to-CPW transitions and two CPW-to-slotline transitions. Fig. 15(a) shows the measured insertion loss for the output power dividing balance between ports 2 and 3 and the measured isolation between ports 1 and 4. The power dividing balance of ± 1 dB has a bandwidth of more than 40% at the center frequency of 3 GHz, and the isolation is greater than 20 dB. Over the same range, a good input and output match is shown in Fig. 15(b) with return loss less than -19 dB. The second peak in return loss shown in Fig. 15(b) is due to the CPW-to-slotline transitions. Fig. 16 shows the phase and power dividing balances between ports 2 and 3. Phase quadrature is maintained at $83° \pm 3°$ over a bandwidth of 45%. The 7° phase error is partly due to fabrication tolerances and misalignments of connectors.

V. Conclusions

New uniplanar hybrid-ring and branch-line couplers were developed. They use coplanar waveguides and slotlines on one side of the substrate. The experimental results of the uniplanar hybrid couplers illustrated superior performances over a broad bandwidth compared to the microstrip and other modified hybrid couplers. With the advantages of broad-band operation, simple design procedure, uniplanar structure, and easy integration with solid-state devices, these new uniplanar hybrid couplers should have many applications in hybrid and monolithic integrated circuits.

References

[1] C.Y. Pon, "Hybrid-ring directional couplers for arbitrary power division," *IRE Trans. Microwave Theory Tech.*, vol. MTT-9, pp. 529–535, Nov. 1961.

[2] E. M. T. Jones, "Wide-band strip-line magic-T," *IRE Trans. Microwave Theory Tech.*, vol. MTT-8, pp. 160–168, Mar. 1960.

[3] L. W. Chua, "New broad-band matched hybrids for microwave integrated circuits," in *Proc. European Microwave Conf.*, 1971, pp. C4/5:1-C4/5:4.

[4] C. H. Ho, L. Fan, and K. Chang, "Ultra wide band slotline hybrid-ring couplers," in *IEEE MTT-S Int. Microwave Symp. Dig.*, 1992, pp. 1175–1178.

[5] D. Kim and Y. Naito, "Broad-band design of improved hybrid-ring 3 dB directional coupler," *IEEE Trans. Microwave Theory Tech.*, vol. MTT-30, pp. 2040–2046, Nov. 1982.

[6] G. F. Mikucki and A. K. Agrawal, "A broad-band printed circuit hybrid-ring power divider," *IEEE Trans. Microwave Theory Tech.*, vol. 37, pp. 112–117, Jan. 1989.

[7] L. Young, "Branch guide directional couplers," in *Proc. Nat. Electron. Conf.*, vol. 12, 1956, pp. 723–732.

[8] J. Reed and G. Wheeler, "A method of analysis of symmetric four-port networks," *IRE Trans. Microwave Theory Tech.*, vol. MTT-4, pp. 246–252, Oct. 1956.

[9] J. Reed, "The multiple branch waveguide coupler," *IRE Trans. Microwave Theory Tech.*, vol. MTT-6, pp. 398–403, Oct. 1958.

[10] L. Young, "Synchronous branch guide directional couplers for low and high power applications," *IRE Trans. Microwave Theory Tech.*, vol. MTT-10, pp. 459–475, Nov. 1962.

[11] R. Levy and L. Lind, "Synthesis of symmetrical branch-guide directional couplers," *IEEE Trans. Microwave Theory Tech.*, vol. MTT-16, pp. 80–89, Feb. 1968.

[12] R. Levy, "Zolotarev branch-guide couplers," *IEEE Trans. Microwave Theory Tech.*, vol. MTT-21, pp. 95–99, Feb. 1973.

[13] M. Muraguchi, T. Yukitake, and Y. Naito, "Optimum design of 3-dB

branch-line couplers using microstrip lines," *IEEE Trans. Microwave Theory Tech.*, vol. MTT-31, pp. 674–678, Aug. 1983.
[14] W. H. Leighton and A. G. Milnes, "Junction reactance and dimensional tolerance effects on X-band −3 dB directional couplers," *IEEE Trans. Microwave Theory Tech.*, vol. MTT-19, pp. 818–824, Oct. 1971.
[15] A. F. Celliers and J. A. G. Malherbe, "Design curves for −3-dB branch-line couplers," *IEEE Trans. Microwave Theory Tech.*, vol. MTT-33, pp. 1226–1228, Nov. 1985.
[16] T. Anada and J. P. Hsu, "Analysis and synthesis of triplate branch-line 3 dB coupler based on the planar circuit theory," in *IEEE MTT-S Int. Microwave Symp. Dig.*, 1987, pp. 207–210.
[17] A. Angelucci and R. Burocco, "Optimized synthesis of microstrip branch-line couplers taking dispersion, attenuation loss and T-junction into account," in *IEEE MTT-S Int. Microwave Symp. Dig.*, 1988, pp. 543–546.
[18] F. C. de Ronde, "A new class of microstrip directional couplers," in *IEEE MTT-S Int. Microwave Symp. Dig.*, 1970, pp. 184–186.
[19] J. A. Garcia, "A wide-band quadrature hybrid coupler," *IEEE Trans. Microwave Theory Tech.*, vol. MTT-19, pp. 660–661, July 1971.
[20] B. Shiek, "Hybrid branch-line couplers—A useful new class of directional couplers," *IEEE Trans. Microwave Theory Tech.*, vol. MTT-22, pp. 864–869, Oct. 1974.
[21] B. Shiek and J. Koehler, "Improving the isolation of 3-dB couplers in microstrip-slotline technique," *IEEE Trans. Microwave Theory Tech.*, vol. MTT-26, pp. 5–7, Jan. 1978.
[22] F. C. de Ronde, "Octave-wide matched symmetrical, reciprocal, 4- and 5- ports," in *IEEE MTT-S Int. Microwave Symp. Dig.*, 1982, pp. 521–523.
[23] R. K. Hoffman and J. Siegl, "Microstrip-slot coupler design, Parts I and II," *IEEE Trans. Microwave Theory Tech.*, vol. MTT-30, pp. 1205–1216, Aug. 1982.
[24] M. Schoenberger, A. Biswas, A. Mortazawi, and V. K. Tripathi, "Coupled slot-strip coupler in finline," in *IEEE MTT-S Int. Microwave Symp. Dig.*, 1991, pp. 751–753.
[25] Y. H. Shu, J. A. Navarro, and K. Chang, "Electronically switchable and tunable coplanar waveguide-slotline band-pass filters," *IEEE Trans. Microwave Theory Tech.*, vol. 39, pp. 548–554, Mar. 1991.
[26] J. A. Navarro, Y. H. Shu, and K. Chang, "Broad-band electronically tunable planar active radiating elements and spatial power combiners using notch antennas," *IEEE Trans. Microwave Theory Tech.*, vol. 40, pp. 323–328, Feb. 1992.
[27] J. A. Navarro, L. Fan, and K. Chang, "The coplanar waveguide-fed electronically tunable slotline ring resonator," in *IEEE MTT-S Int. Microwave Symp. Dig.*, 1992, pp. 951–954.
[28] C. H. Ho, L. Fan, and K. Chang, "Broad-band uniplanar hybrid-ring coupler," *Electron. Lett.*, vol. 29, pp. 44–45, Jan. 1993.
[29] T. Hirota, Y. Tarusawa, H. Ogawa, and K. Owada, "Planar MMIC hybrid circuit and frequency converter," in *IEEE MTT-S Int. Microwave Symp. Dig.*, 1986, pp. 103–105.
[30] T. Hirota, Y. Tarusawa, and H. Ogawa, "Uniplanar MMIC hybrids—A proposed new MMIC structure," *IEEE Trans. Microwave Theory Tech.*, vol. MTT-35, pp. 576–581, June 1987.
[31] M. Aikawa and H. Ogawa, "Double-sided MIC's and their applications," *IEEE Trans. Microwave Theory Tech.*, vol. 37, pp. 406–413, Feb. 1989.
[32] T. Tokumitsu, S. Hara, and M. Aikawa, "Very small, ultra-wide-band MMIC magic-T and applications to combiners and dividers," in *IEEE MTT-S Int. Microwave Symp. Dig.*, 1989, pp. 963–966.
[33] ——, "Very small ultra-wide-band MMIC magic-T and applications to combiners and dividers," *IEEE Trans. Microwave Theory Tech.*, vol. 37, pp. 1985–1990, Dec. 1989.
[34] S. B. Cohn, "Slot line on a dielectric substrate," *IEEE Trans. Microwave Theory Tech.*, vol. MTT-17, pp. 768–778, Oct. 1969.
[35] J. B. Knorr, "Slot-line transitions," *IEEE Trans. Microwave Theory Tech.*, vol. MTT-22, pp. 548–554, June 1974.
[36] B. Schupert, "Microstrip/slotline transition: Modeling and experimental investigations," *IEEE Trans. Microwave Theory Tech.*, vol. 36, pp. 1272–1282, Aug. 1988.
[37] B. Shiek and J. Kohler, "An improved microstrip to microslot transition," *IEEE Trans. Microwave Theory Tech.*, vol. MTT-24, pp. 231–233, Dec. 1976.
[38] N. Marchand, "Transmission line conversion transformers," *Electronics*, vol. 17, pp. 142–145, Dec. 1944.
[39] G. Oltmann, "The compensated balun," *IEEE Trans. Microwave Theory Tech.*, vol. MTT-14, pp. 112–119, Mar. 1966.
[40] V. H. Hanna and L. Rambroz, "Broad-band planar coplanar waveguide-slotline transition," in *Proc. 12th European Microwave Conf.*, 1982, pp. 628–631.
[41] H. Ogawa and A. Minagawa, "Uniplanar MIC balanced multiplier—A proposed new structure for MIC's," *IEEE Trans. Microwave Theory Tech.*, vol. MTT-35, pp. 1363–1368, Dec. 1987.
[42] D. Cahana, "A new coplanar waveguide/slotline double-balance mixer," in *IEEE MTT-S Int. Microwave Symp. Dig.*, 1989, pp. 967–968.
[43] V. Trifunovic and B. Jokanovic, "New uniplanar balun," *Electron. Lett.*, vol. 27, pp. 813–815, May 1991.
[44] T. Q. Ho and S. M. Hart, "A novel broad band coplanar waveguide to slotline transition," *IEEE Microwave Guided Wave Lett.*, vol. 2, pp. 415–416, Oct. 1992.
[45] H. Y. Lee and T. Itoh, "Wide-band and low return loss coplanar strip feed using intermediate microstrip," *Electron. Lett.*, vol. 24, pp. 1027–1028, Sept. 1988.
[46] R. G. Manton, "Hybrid networks and their uses in radio-frequency circuits," *Radio Electron. Eng.*, vol. 54, pp. 473–489, 1984.
[47] K. Chang, *Handbook of Microwave and Optical Components, Vol. 1*. New York: Wiley, 1990, pp. 145–150.

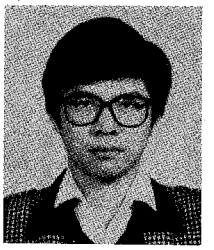

Chien-Hsun Ho was born in Kaohsung, Taiwan, on October 9, 1963. He received the B.S. and M.S. degrees in electrical engineering from National Taiwan University, Taipei, Taiwan, in 1985 and 1987, respectively.

Since 1990 he has been working as a Research Assistant in the Microwave Lab, Department of Electrical Engineering, Texas A&M University, College Station. Currently, he is working toward the Ph.D. degree. His research interests include uniplanar coupler designs, optically controlled microwave devices, waveguide filters, and MMIC designs.

Lu Fan received the B.S. degree in electrical engineering from Nanjing Institute of Technology (now Southeast University), Nanjing, China, in 1982.

From September 1982 to December 1990 he was with the Department of Radio Engineering, Nanjing Institute of Technology, as a Teaching Assistant and Lecturer. In January 1991 he became a Research Associate in the Department of Electrical Engineering, Texas A&M University, College Station. His research interests include microwave and millimeter-wave components and circuits.

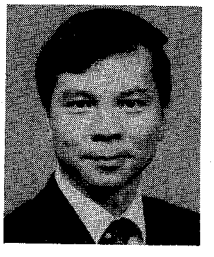

Kai Chang (S'75–M'76–SM'85–F'91) received the B.S.E.E. degree from the National Taiwan University, Taipei, Taiwan, the M.S. degree from the State University of New York at Stony Brook, and the Ph.D. degree from the University of Michigan, Ann Arbor, in 1970, 1972, and 1976, respectively.

From 1972 to 1976 he worked for the Microwave Solid-State Circuits Group, Cooley Electronics Laboratory, University of Michigan, as a Research Assistant. From 1976 to 1978 he was employed by Shared Applications, Inc., Ann Arbor, where he worked in

computer simulation of microwave circuits and microwave tubes. From 1978 to 1981 he worked for the Electron Dynamics Division, Hughes Aircraft Company, Torrance, California, where he was involved in the research and development of millimeter-wave solid-state devices and circuits, power combiners, oscillators, and transmitters. From 1981 to 1985 he worked for the TRW Electronics and Defense, Redondo Beach, CA, as a Section Head, developing state-of-the-art millimeter-wave integrated circuits and subsystems including mixers, VCO's, transmitters, amplifiers, modulators, upconverters, switches, multipliers, receivers, and transceivers. He joined the Electrical Engineering Department of Texas A&M University in August 1985 as an Associate Professor and was promoted to a Professor in 1988. In January 1990 he was appointed E-Systems Endowed Professor of Electrical Engineering. His current interests are in microwave and millimeter-wave devices and circuits, microwave integrated circuits, microwave optical interactions, and antennas.

Dr. Chang served as the Editor of the four-volume *Handbook of Microwave and Optical Components* (New York: Wiley, 1989, 1990). He is the Editor of the Microwave and Optical Technology Letters and the Wiley Book Series in Microwave and Optical Engineering. He has published over 200 technical papers and several book chapters in the areas of microwave and millimeter-wave devices and circuits. He received the Special Achievement Award from TRW in 1984, the Halliburton Professor Award in 1988, the Distinguished Teaching Award in 1989, and the Distinguished Research Award in 1992 from the Texas A&M University.